Analysis of the suitability of using the selected wind turbine blades for wind power appliances based on numerical analyses

Krzysztof Pytel[1,*], *Szymon* Szpin[1], *Wiktor* Hudy[2], *Małgorzata* Piaskowska–Silarska[2], and *Stanisław* Gumuła[1]

[1]AGH University of Science and Technology, Department of Power Systems and Environmental Protection Facilities, Mickiewicza 30 Av. 30-065 Cracow, Poland
[2]Pedagogical University of Cracow, Podchorążych 2, 30-084 Cracow, Poland

Abstract. The aim of this study was a comparative analysis of the suitability of the use of airfoil for wind power. Based on numerical analyses and analytical methods, information on the power factor was obtained. The analyses were carried out for the wind turbine blades and rotors of a vertical axis wind turbine. The tests were performed for the constructed profile and compared with the profile DU 06-W-200 used in the construction of a wind turbine rotors. A vertical axis wind turbine model equipped with designed blade profiles was prepared. The main predicted purpose of the device is to supply electricity to the household. The blade profile models were prepared and then a numerical analysis was performed using the CFD application. The obtained results for given wind speeds and types of profiles were compared with each other. The conducted research allowed to determine the sense of applying the unaudited profile based on the determined value of wind turbine power coefficient. Studies have shown that the accurate preparation of the optimal rotor blade with respect to flow of air stream strongly influences the characteristics of the wind turbine.

1 Introduction

One of the most important issues appearing in the power energy sector is development and examining of modern technologies enabling maximization of obtaining energy from renewable sources. Pollution resulting from burning fossil fuels in conventional power plants have become a serious ecological and economic problems in the whole world [1 – 3]. The development of appropriate technology to intensify the use of renewable energy sources in this context is very important [4].

Wind power plants, are most often associated with large high masts and turbines with blades of an enormous span. This is not the only solution for wind turbines. The result is the construction and continuous development of vertical axis wind turbines. Technology of wind turbines with a vertical axis of rotation is a technology that tries to convince investors to back to that idea. Technical parameters are promising. A turbine of this type can work with very

---

* Corresponding author: kpytel@agh.edu.pl

low wind speed. The design allows the investor to achieve a sufficiency high efficiency without the need to build high masts and allows the facility to be assembled from functional segments [5–7]. An additional advantage may be the long working period of the device. A vertical axis wind turbine (VAWT) works well enough in urban areas. A classic horizontal axis wind turbine (HAWT) are sensitive to an air turbulence and can be a source of noise. The VAWT can be used as a energy source for powering single-family houses, campsites and summerhouses, yachts, measuring and signalling devices, advertising banners, street lamps. VAWT can be used wherever access to a standard power grid is difficult or impossible. The main element of the wind power plant is the rotor converting wind energy into mechanical energy. The rotor is mounted on a low-speed shaft and rotates mostly at a speed of 15 to 180 rpm. This speed is multiplied by the transmission and transferred to the generator using a high-speed shaft. The generator produces electricity from mechanical energy [8,9].

Design requirements for modern turbines are high. New, advanced technologies, light and durable materials and the ability to perform complex aerodynamic simulations give designers great opportunities to create modern airfoils and efficient turbines. The operation of the wind turbine is based on the use of lift and drag forces. Wind power generators designed to start up at low wind speeds and high functionality are just a few of the advantages of the Darrieus type wind turbine. Despite not very complicated construction, such a power plant allows you to react to wind from any direction. Despite the disadvantage of this turbine associated with a very small starting torque, such a power plant with a low rotational rotor speed is characterized by a lower noise propagation during machine operation and the possibility of mounting closer to the population centres. Wind turbines constructed today are based on the achievements of aviation technology (Fig. 1a) and the production of wind turbine components has a lot in common with the aviation industry. These similarities mainly concern operating conditions, which in both cases take place at variable wind speeds and directions [10, 12]. Both in an aviation as well as in a wind power engineering, the geometry of the blade has a decisive impact on characteristics of the wind turbine or an aircraft performance. The changes in a surface smoothness and a shape of the airfoil are of great importance and can cause significant differences in the performance of the power plant with the same dimensions of the blades. Even slight differences in a shape can significantly change the characteristics. Therefore, choosing the right rotor blade is very important, and properly profiled blades guarantee a higher efficiency of the conversion of kinetic energy of wind into mechanical energy of the rotor [13 – 15].
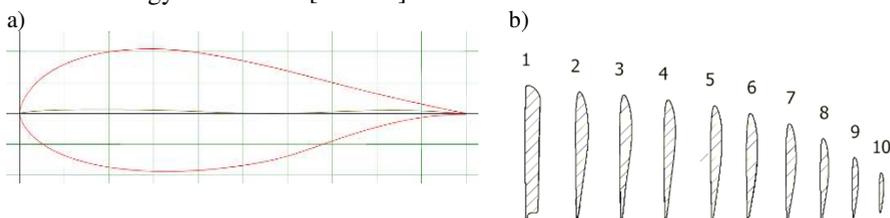

Fig. 1. Airfoils; (a) the DU 06-W-200 rotor blade profile used in the construction of wind turbines; (b) the designed rotor blade profile

Airfoils are characterized by an efficient work even with very large Reynolds numbers of 150.000 and 700.000. The increased blade width allows power plants to maintain the assumed capacity in a greater range of wind speed. Due to the thickening of the profiles, it is possible to obtain a higher strength of the structure.

A new wind turbine blade has been modelled (Fig.1b). Assuming that each cross-section of the blade behaves like a profile in a two-dimensional flow field, the rotor has been analysed in a simplified manner (Tab.1). In fact, it is impossible to use the total wind power. In

practice, it turns out that only part of the wind power is actually used to set the turbine in motion. The mechanical power of a wind turbine is obtained by reducing the wind power by the power coefficient C_p.

Table 1. Assumptions for calculations

Airfoil	New blade	DU 06-W-200
c – chord length	105 mm	100 mm
H – max thickness	440 mm	445 mm
N_b – number of blades	3	3
R_z – radius of rotor	250 mm	250 mm
D – diameter of rotor	500 mm	500 mm
v – wind speed	$5 - 25\frac{m}{s}$	$5 - 25\frac{m}{s}$
rated wind speed	$v_{rated} = 12\frac{m}{s}$	$v_{rated} = 12\frac{m}{s}$
start-up wind speed	$v_{min} = 5\frac{m}{s}$	$v_{min} = 5\frac{m}{s}$
max wind speed	$v_{max} = 25\frac{m}{s}$	$v_{max} = 25\frac{m}{s}$
shape		
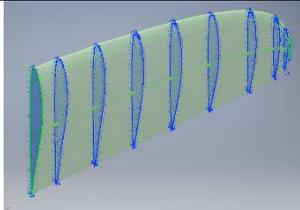
Thus, the energy on the rotor shaft is calculated as follows:

$$E = \frac{1}{2}v^3 \cdot A \cdot C_p \tag{1}$$

where :

C_p	–	power coefficient,
P	–	power, W,
ρ	–	density of air, kg/m^3,
v	–	wind speed, m/s,
A	–	area of a rotor, m2, given by: A=πR^2.

a)   b)
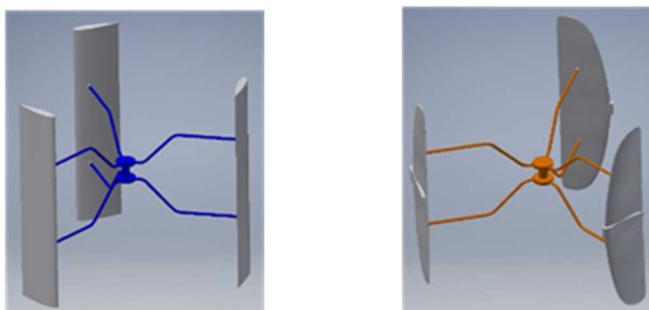
Fig. 2. Wind turbine model for numerical analysis; (a) with DU-06-W-200 profiles; (b) with designed airfoils

The profile DU-06-W-200 based on the data [16] and the new designed airfoil were modelled. The results obtained during the numerical analysis were referenced to these profiles. The modelled blade made it possible to obtain the final version of the turbine, which was used during the numerical analysis (Fig. 2a, 2b).

2 Power coefficient calculations

The value of the power coefficient C_p depends on the speed of the air before and after the rotor. The velocity of the air stream entering the rotor and the air velocity after the rotor is expressed as v_1 and v_2, respectively. Three analytical methods of calculating the power coefficient C_p are presented.

The Betz limit is a hypothetical boundary on the total amount of power that could be extracted by a wind turbine from a wind movement [17 – 19]. In the first method power coefficient C_p using the Betz limit is calculated as follows:

$$C_p = \frac{1}{2}\left[1 - \left(\frac{v_2}{v_1}\right)^2\right] \cdot \left[1 + \frac{v_2}{v_1}\right] \qquad (2)$$

where :

    v_1 –   speed of the air stream entering the rotor, m/s,
    v_2 –   air speed behind the rotor, m/s.

Based on the above formula, a plot of C_p coefficient depending on the air speed was prepared (Fig. 3a). Calculated power coefficient values reach in reality, in fact, lower values due to the occurrence of various types of aerodynamic losses.
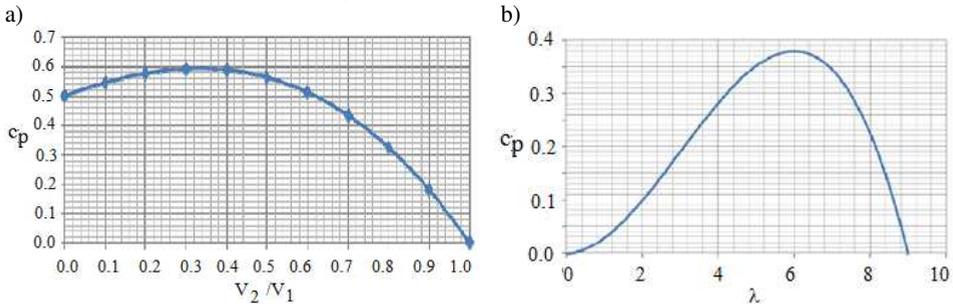
Fig. 3. Power coefficient C_p of wind turbine based on analytical analyses; (a) as a function of wind speed V_2/V_1 (Betz limit); (b) as a function of TSR λ;

The second method enabling the determination of the power coefficient C_p is based on the tip speed ratio (TSR) λ, which makes the rotational angular velocity dependent on the wind speed [15, 21, 22]:

$$\lambda = \frac{R_z \Omega}{V_1} \qquad (3)$$

where :

    Ω –   angular velocity of the rotor wheel, rad/s,
    v_1 –   wind speed, m/s,
    R_z –   external radius of the impeller, m.

The rotational speed of the rotor can be express as $\Omega = (\pi n)/30$, where *n* is a rotor speed, rpm.

It is possible to find a relationship between C_p and TSR:

$$C_p = \left(\frac{3C_{p,max}}{\lambda_{max}^2}\right) \cdot \lambda^2 - \left(\frac{2C_{p,max}}{\lambda_{max}^3}\right) \cdot \lambda^3 \qquad (4)$$

where :

    λ –   TSR,
    λ_{max} –   maximum TSR,
    $C_{p,max}$ –   maximum power coefficient.

Based on the above formula, a plot of C_p depending on the TSR was prepared (Fig. 3b).

The third method of determining the power coefficient is based on specific aerodynamic coefficients of the wind turbine rotor blades. This method is especially useful for comparison of a turbine performance with different number of blades [15, 23] and it can be presented as:

$$C_p = \frac{16}{27}\left(1 - \frac{C_1}{N \cdot \lambda}\right)^2 \cdot \left(e^{\frac{-C_2}{\lambda^{1.29}}} - \frac{C_d}{C_l} \cdot \lambda\right) \tag{5}$$

where :

N	–	a number of wind turbine blades,
λ	–	a TSR,
C_1, C_2	–	coefficients, in the literature they appear in a simplified form $C_1 = 0.416$ and $C_2 = 0.35$,
C_d	–	a drag coefficient,
C_l	–	a lift-coefficient.

Based on the above analyses, the power coefficient (C_p) can be the measure of the wind turbine rotor efficiency at a given wind speed, and it provides an approximation of the actual power produced by the rotor of the wind turbine.

3 Experimental procedure

The aim of the research is to determine the impact of the setting of the rotor axis on the power coefficient. Moreover, the role of optimal shape of the blades of the wind power plant was specified. Based on the computational algorithm and following the similar solutions found in the technique, the rotational speeds of the wind turbine rotor have been determined [15, 21, 23].
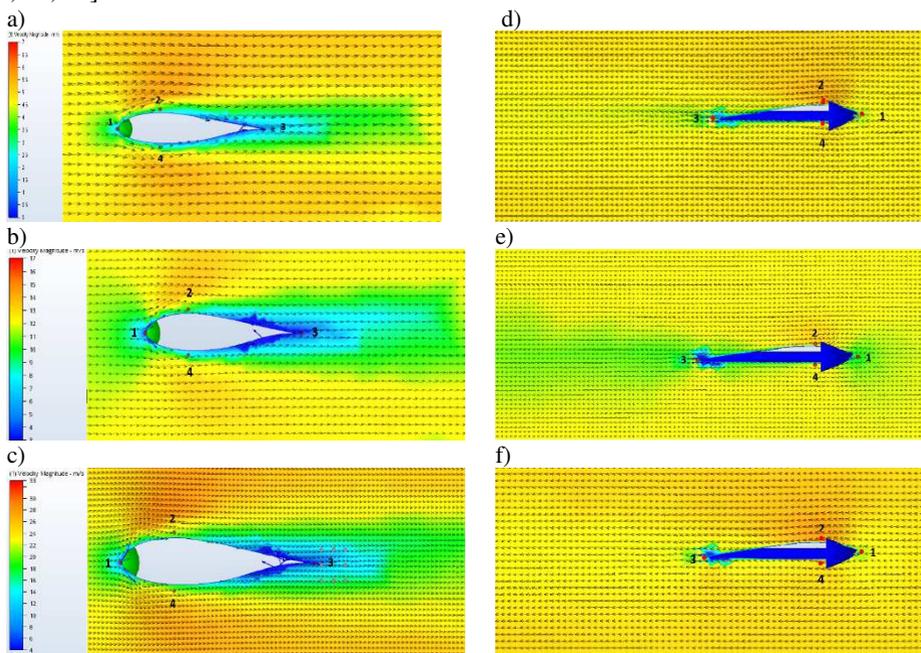
Fig. 4. The distribution of air speed for DU 06-W-200 and designed blade profile at different speeds of the airflow: (a) DU 06-W-200 at air speed 5 m/s; (b) DU 06-W-200 at air speed 12 m/s; (c) DU 06-W-200 at air speed 25 m/s; (d) designed blade at air speed 5 m/s; (e) designed blade at air speed 12 m/s; (f) designed blade at air speed 25 m/s.

The analysis was carried out at three rotational speeds of rotor depending on three wind speeds: minimum, rated and maximum wind speed. Minimum speed of the turbine describes a rotational speed of the rotor at which the turbine can start automatically. Rated rotational speed describes the rotor speed at which the wind turbine should achieve the nominal power.

Maximum speed describes the rotor speed at which the turbine can operate safely, without exposing the rotor structure to the destructive effect of centrifugal forces, vibrations and other factors that can damage the turbine rotor.

Considering that researches conducted on similar types of the wind turbines showed that constant-geometry Darrieus turbines can start-up during wind gusts and work at wind speeds of even 2- 5 m/s, the minimum wind velocity has been assumed as v_{min}=5 m/s.

Considering similar technical applications presented on the market by turbine manufacturers, taking into account the strength aspects and the correct and safe operation of the turbine structure, the maximum wind speed was assumed at the level of v_{max}=25 m/s, and the rated wind speed at the level v_{znam}=12 m/s.

Analyses were prepared for chosen rotor blades (Fig. 4). The speed of the moving air is shown using graphical vectors illustrating the distribution of airflow velocity and measured at four characteristic measuring points. The air speed values read from the measurement points at given air speeds are listed in the table (Tab.2, 3).
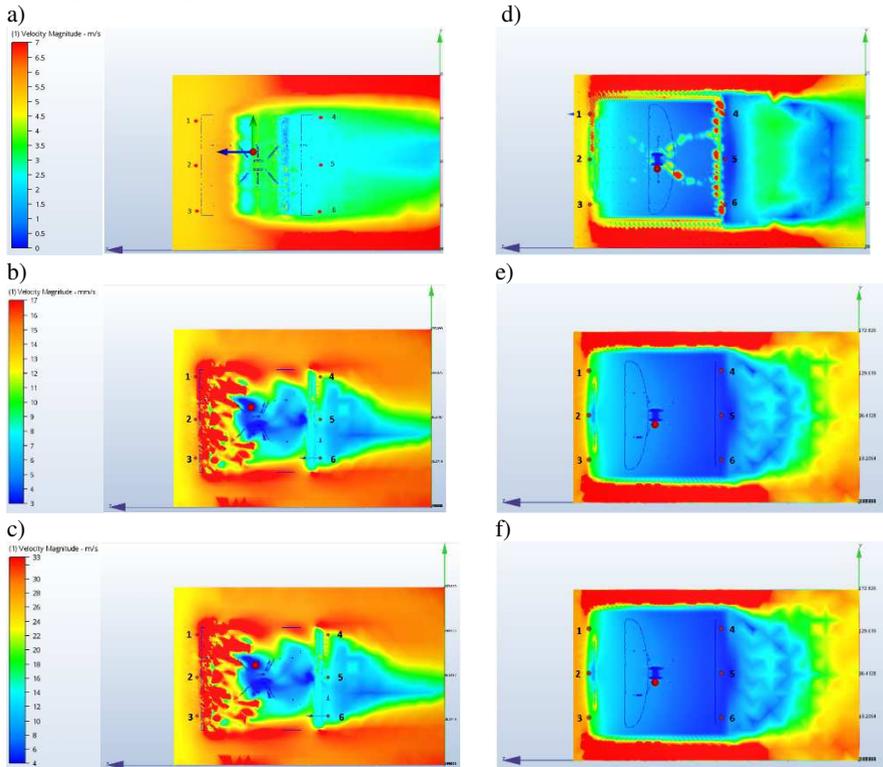
Fig. 5. The distribution of air speed for DU 06-W-200 and designed blade profile at different speeds of the airflow: (a) DU 06-W-200 at air speed 5 m/s; (b) DU 06-W-200 at air speed 12 m/s; (c) DU 06-W-200 at air speed 25 m/s; (d) designed blade at air speed 5 m/s; (e) designed blade at air speed 12 m/s; (f) designed blade at air speed 25 m/s.

In the same way as in the case of the tested blades profiles, a volume was generated, materials were assigned for the generated volume and turbine models, and the boundary conditions of the analyzes were determined. As for the blade profiles, the following: 5 m/s, 12 m/ s and 25 m/s air velocities were assumed: The rotor has been given a motion with a

constant angular velocity. The appropriate angular velocities, determined on the basis of the air flow value, were imposed on the specified axis and the center of rotation (the turbine hub).

The following angular velocities were adopted: 63 1/s, 145 1/s and 310 1/s. The visible color difference between the upper and lower side of the profile (Fig. 5) results from the difference in speed and pressures. The lift force acting on the rotor blades and setting it in motion is formed as a result of these differences. Analyses were conducted for DU 06-W-200 and new designed blade profile.

The speed of the moving air is shown using graphical vectors illustrating the distribution of airflow velocity and measured at four characteristic measuring points. The air speed values read from the measurement points at given air speeds are listed in the table (Tab.4, 5).

Table 2. Airflow velocities for the DU 06-W-200 profile at four characteristic points

point	air speed before blade, m/s	measured air speed, m/s	air speed before blade, m/s	measured air speed, m/s	air speed before blade, m/s	measured air speed, m/s
1	5	0.83	12	2.09	25	4.56
2	5	3.37	12	8.97	25	21.95
3	5	0.89	12	2.00	25	4.38
4	5	3.25	12	8.65	25	17.01

Table 3. Airflow velocities for the designed blade profile at four characteristic points

point	air speed before blade, m/s	measured air speed, m/s	air speed before blade, m/s	measured air speed, m/s	air speed before blade, m/s	measured air speed, m/s
1	5	3.24	12	9.23	25	21.34
2	5	5.95	12	14.45	25	30.24
3	5	1.67	12	4.21	25	8.09
4	5	4.86	12	12.06	25	25.39

Table 4. Airflow velocities for the rotor made of DU 06-W-200 profile at six characteristic points

point	air speed before blade, m/s	measured air speed, m/s	air speed before blade, m/s	measured air speed, m/s	air speed before blade, m/s	measured air speed, m/s
1	5	4.75	12	17.45	25	26.54
2	5	4.86	12	16.85	25	27.52
3	5	4.69	12	14.93	25	27.14
4	5	1.84	12	11.84	25	17.92
5	5	1.75	12	7.78	25	15.68
6	5	1.83	12	8.93	25	20.41

Table 5. Airflow velocities for the rotor made of designed blade profile at six characteristic points

point	air speed before blade, m/s	measured air speed, m/s	air speed before blade, m/s	measured air speed, m/s	air speed before blade, m/s	measured air speed, m/s
1	5	6.81	12	12.5	25	27.32
2	5	7.23	12	10.9	25	25.11
3	5	5.82	12	13.4	25	26.53
4	5	1.25	12	8.3	25	8.32
5	5	2.74	12	7.2	25	6.45
6	5	3.52	12	7.5	25	11.21

4 Determination of values of power coefficient by analytical methods

For averaged measurements of air flow velocities collected at the measuring points before and after the turbine, the value of the power coefficient C_p was determined. The value of C_p

coefficients is calculated taking into accout Betz limit in succession for v_{min}=5$[\frac{m}{s}]$, v_{rated}=12$[\frac{m}{s}]$ and v_{max}=25$[\frac{m}{s}]$ (Tab. 6).

Table 6. Values of C_p coefficients at three different flow rates

blades	C_p at V_{min}=5 m/s	C_p at V_{rated}=12 m/s	C_p at V_{max}=25 m/s
DU-06-W-200	0.242872	0.265886	0.196005
new designed	0.246465	0.251948	0.299166

On the basis of the range of the power coefficient can be concluded that results are possible to obtain.

While determining the value of the Cp coefficient with the use of the tip speed ratio, for the tested type of turbines, the maximum value of the power coefficient $C_{p, max}$=0.35 was assumed. The maximum TSR λ_{max}=6.4 and TSR λ=3.15 were assumed. In this method, identical results were obtained for all types of analyzed turbines. The distinguishing feature of TSR is dependent on the rotational speed, which has been adopted for all types of turbines as the same. In addition, in all types of rotors, the same radius of rotor was assumed, and in addition, this analysis was carried out with identical air flow conditions.

$$C_p = \left(\frac{3 \cdot 0.35}{6.4^2}\right) \cdot 3.15^2 - \left(\frac{2 \cdot 0.35}{6.4^3}\right) \cdot 3.15^3 = 0.171 \tag{6}$$

The value of the power coefficient calculated for this type of wind turbines, taking into account the adopted dimensions and parameters, was equal to : $C_p = 0.171$.

While determining the value of the Cp coefficient with the use of the aerodynamic coefficients, for the tested type of turbines, the values of the lift force was determined by determining the value of the lift and drag force coefficients. Based on the assumptions: the number of wind turbine blades N=3, the TSR as λ=3.15 and coefficients C_1=0.416 and C_2=0.35, for the new profile we calculate:

- for the air speed $v_{min} = c_{\infty 1} = 5 \left[\frac{m}{s}\right]$

$$C_{p1} = \frac{16}{27}\left(1 - \frac{0.416}{3 \cdot 3.15}\right)^2 \cdot \left(e^{3.15\frac{-0.35}{1.29}} - \frac{0.2309}{0.1027} \cdot 3.15\right) = 0.1547 \tag{7}$$

- for the air speed $v_{rated} = c_{\infty 2} = 12 \left[\frac{m}{s}\right]$

$$C_{p1} = \frac{16}{27}\left(1 - \frac{0.416}{3 \cdot 3.15}\right)^2 \cdot \left(e^{3.15\frac{-0.35}{1.29}} - \frac{0.1796}{0.1876} \cdot 3.15\right) = 0.2965 \tag{8}$$

- for the air speed $v_{max} = c_{\infty 3} = 25 \left[\frac{m}{s}\right]$

$$C_{p1} = \frac{16}{27}\left(1 - \frac{0.416}{3 \cdot 3.15}\right)^2 \cdot \left(e^{3.15\frac{-0.35}{1.29}} - \frac{0.1701}{0.2213} \cdot 3.15\right) = 0.3451 \tag{9}$$

The values of the power coefficient for the turbine with the DU 06-W-200 profiles were calculated. The Cp coefficients for the analyzed profiles, determined by three methods, are compared (Tab. 7).

Table 7. Values of C_p coefficients at three different calculation

blades	C_p at Betz limit	C_p at TSR	C_p at aero. coefficients	C_p average
DU-06-W-200	0.2659	0.1710	0.2240	0.2203
new designed	0.2519	0.1710	0.2965	0.2398

According to the first calculation method, the Cp coefficients for the turbine with the new designed blade profile is slightly worse to the comparative rotor.

The second method gave the same result for all types of analyzed rotors. This method depends on the type of turbine and its dimensions (diameter of the rotor wheel, the number of blades in the rotor), and do not depend on the parameters of the rotor's motion or the type of profiles used.

In the third method, better results ware obtained for the turbine with a new designed blade profile, and also the arithmetic average of all methods, calculated for each type of profile, indicate the new designed profile as better sollution.

5 Conclusion

A wind farm with a vertical axis of rotation is a simple construction that gives the possibility of obtaining electricity in places where access to it is limited or impossible. A model of a wind turbine with a vertical axis of rotation was developed with the use of new profiles. In order to interpret the obtained results and reference to reality, for comparative analysis the comparative profile DU 06-W-200 and the turbine with their use were used.

Based on the numerical analysis, it can be concluded that the new profile achieves comparable or even better results than the comparative profile in relation to the aerodynamics itself and the value of wind power used by the turbine.

The CFD analysis of the flow around the profiles showed a greater difference in speed between the air speeds at the bottom and the back of the blade for the designed profile, which suggests the creation of more lift force.

Also based on the power coefficient C_p determined by three methods, it is possible to suggest to use the new profile in the technology. The average arithmetic value of the C_p coefficient calculated on the basis of the above methods gives a better result for the designed blade profile than currently use one.

However, in addition to the properly engineered power plant blade, there are still many elements affecting the efficiency of the turbine: the structural parameters of the wind power plant, drives and control systems, materials from which the power plant was built, elements of the climate [24–27]. In order for the investment to bring profit to investors, each of these factors must have a positive impact on the venture.

References

1. S. Gumula, W. Hudy, M. Piaskowska–Silarska, K. Pytel, Chemical Industry, **94,** pp. 1000–1003, (2015)
2. H. Noga, Information technologies and technical education, **1,** pp. 165–169, (2009)
3. I. Turekova, J. Depesova, A. Haskova, T. Bagalova, EDULEARN 15 (2015) 1913–1921.
4. A. Bianchini, G. Ferrara, L. Ferrari, Energy Conversion and Management, **89**, pp. 690-707, (2015)
5. T. Prauzner, Electrotechnical overview, **88,** pp. 205–208, (2012)
6. J. Suchanicz, G. Stopa, J. Kusz, M. Zubko, W. Hofmeister, M. Antonova, A. Kalvane, M. Dambekalne, A. Sternberg, I. Jankowska-Sumara, B. Garbarz-Glos, D Wcisło, K. Konieczny, K. Pytel, A. Finder, Journal of Materials Science, **45,** pp. 1453–1458, (2010)
7. P. Dulian, B. Garbarz-Glos, W. Bąk, M. Antonova, C. Kajtoch, K. Wieczorek-Ciurowa, H. Noga, Ferroelectrics, **497**, pp. 62–68, (2016)
8. S. Gumula, K. Pytel, M. Piaskowska-Silarska, Polish Journal of Environmental Studies, **23**, pp. 2315–2320, (2014)
9. W. Hudy, K. Jaracz. K. Pytel, *International Carpathian Control Conference*, **16,** pp. 81-185, (2015)
10. M. L. Niculescu, M. G. Cojocaru, M. V. Pricop, D. Pepelea, A. Dumitrache, D. E. Crunteanu, *AIP Conference Proceedings*, **1863,** 420003, (2017)
11. L. Borowik, P. Ptak, Przeglad Elektrotechniczny, **88**, pp. 142–145, (2012)
12. G. Ronsten, Journal of Wind Engineering and Industrial Aerodynamics, **39**, 1, pp. 105-118, (1992)
13. Chen, Jin, et al. Applied Mathematical Modelling, **40**, 3, pp. 2002–2014, (2016)
14. Spinato, F., et al. "Reliability of wind turbine subassemblies." IET Renewable Power Generation, **3**, 4, pp. 387–401, (2009)
15. D. Mazur, Strength calculations and vibrations of the Darrieus type turbine, Rzeszow, PR, (2012)

16. http://airfoiltools.com, access June 1st, (2018)
17. S. Gumula, K. Pytel, M. Piaskowska–Silarska, Polish Journal of Environmental Studies, **23**, pp. 2321–2325, (2014)
18. K. Pytel, W. Hudy, H. Noga, W. Kulinowski, *International Carpathian Control Conference*, **17**, pp. 401–406, (2016)
19. K. Pytel, W. Hudy, H. Noga, W. Kulinowski, *International Carpathian Control Conference*, **17**, pp. 407–412, (2016)
20. S. Gumuła, T. Knap, Determination of the optimal geometry and movement parameters of the wind power plants depending on the average annual wind speed. *National Forum "Small Energy - '97."* Zakopane (1997)
21. S.Gumuła, Wind Energy, Kraków, AGH, (2006)
22. R. Jablonski, M. Turkowski, R. Szewczyk (Eds.). *Recent Advances in Mechatronics. Proceedings of 7th International Symposium Mechatronics held Sept. 19–21 in Warsaw*, Poland. (2007)
23. F.D. Bianchi, H. de Battista, R.J. Hernán, Wind Turbine Control Systems. Principles, Modelling and Gain Scheduling Design, Springer, (2007)
24. B. Garbarz-Glos, W. Bąk, H. Noga, M. Antonova, A. Kalvane, W. Śmiga, Integrated Ferroelectrics, **173**, pp. 12–18, (2016)
25. W. Śmiga, B. Garbarz-Glos, W. Piekarczyk, H. Noga, D. Sitko, M. Karpierz, M. Livinsh, Integrated Ferroelectrics, **173**, pp. 46–52, (2016)
26. W. Hudy, M. Piaskowska-Silarska, K. Pytel, S. Gumuła, Archives of Mining Sciences, **62**, pp. 579-596, (2017)
27. D. Olszewska, T. Prauzner, P. Ptak, H. Noga, Przegląd Elektrotechniczny, **12**, pp. 191-193, (2016)